

# Structural Analysis of Nano-sized Iron Oxide Particles Prepared by Vacuum Evaporation Technique

Hiroshi Yanagimoto, Shigehito Deki\* and Kazuo Gotoh\*\*

Division of Molecular Science, The Graduate School of Science and Technology, Kobe University,  
Rokkodai-cho, Nada-ku, Kobe 657-8501, Japan

Fax: 81-78-803-6160, e-mail: yanagimoto@cx2.cx.kobe-u.ac.jp

\*Department of Chemical Science and Engineering, Faculty of Engineering, Kobe University,  
Rokkodai-cho, Nada-ku, Kobe 657-8501, Japan

Fax: 81-78-803-6186, e-mail: deki@kobe-u.ac.jp

\*\*Engineer Application Research Sect., Research and Development Division, Mitsuboshi Belting, Ltd.,  
Hamazoe-dori, Nagata-ku, Kobe 653-0024, Japan

Fax: 81-78-671-7516, e-mail: rd\_appli@mitsuboshi.co.jp

Nano-sized  $\text{Fe}_2\text{O}_3$  particles have been successfully prepared by vacuum evaporation of iron onto a molten  $\text{NH}_2$ -terminated poly(ethylene oxide) film. The  $\text{Fe}_2\text{O}_3$  particles exhibited well-dispersion below *ca.* 10 wt% of  $\text{Fe}_2\text{O}_3$  content in the composite. The structure of  $\text{Fe}_2\text{O}_3$  particles obtained was characterized by HRTEM, electron diffraction, XPS and XRD, and it emerged that  $\alpha$ - and  $\gamma$ - $\text{Fe}_2\text{O}_3$  particles coexist in the matrix film. The morphological change of  $\text{Fe}_2\text{O}_3$  particles with heat treatment and the change of their optical property have been discussed. The particle with relatively narrow size distribution was changed from 1.3 nm to 3.4 nm in sizes with heat treatment, and the absorption edge evaluated from optical absorption spectra for  $\text{Fe}_2\text{O}_3$  particles shifted to longer wavelength.

Key words: nanoparticles,  $\text{Fe}_2\text{O}_3$ , structural analysis,  $\text{NH}_2$ -terminated poly(ethylene oxide)

## 1. INTRODUCTION

In recent years, the preparation, characterization, and applications of nano-sized metal oxide particles have been subject of intense study in various fields, *e.g.*, chemistry, physics, material science, biology, and the corresponding engineering [1-3]. Since these particles usually exhibit unique electronic, optical, magnetic, and chemical properties significantly different from those of the bulk materials due to their reduced dimensions, especially less than 10 nm in size, they have potential materials for various applications such as catalysis, optical and electronic devices, magnetic storage media, and drug delivery [4-7]. Of special interest are nano-sized iron oxide particles as they retain important position in magnetic materials [8-12].

A large number of methods have been reported for the preparation of nano-sized metal oxide particles, *e.g.*, sol-gel method [13], chemical oxidation in micellar media or in mineral or polymer matrices [14] and flame pyrolysis [15]. Their final goal is to prepare monodispersed metal oxide particles not only at high concentration but also with uniform dispersion as well as to control their size precisely in nanometer regime. However, there are few reports on successful method fulfilled these requests.

We have previously reported on preparation of gold [16] or cuprous oxide [17] particles dispersed in  $\text{NH}_2$ -terminated poly(ethylene oxide) (PEO- $\text{NH}_2$ ) film through simple route that metal counterparts were vacuum-evaporated onto a molten PEO- $\text{NH}_2$  film and, if necessary, following heat treatment. By the successful preparation method, we can prepare well-dispersed particles with small size in nanometer regime. The interaction between the particles and - $\text{NH}_2$  end groups of the matrix molecule has proven to be responsible for the uniform dispersion [17].

This article describes the preparation and

characterization of nano-sized iron oxide particles in PEO- $\text{NH}_2$  film by vacuum evaporation of metallic iron. Well-known characteristics of the iron oxide are a variety of possible interconversions between the different phases [18, 19]. Therefore, we especially focus on the structure of the particles. The morphological and structural characterizations of the particles have been performed by means of transmission electron microscopy (TEM), X-ray photoelectron spectroscopy (XPS) and X-ray diffraction (XRD). The content of the particles and thermal stability of the composite were studied through thermogravimetry-differential thermal analysis (TG-DTA) and Fourier transform infrared (FT-IR) spectroscopy. The morphological changes of nano-sized iron oxide particles with post-heat treatment and the change of the optical property are also discussed.

## 2. EXPERIMENTAL

The polymeric matrix films with a thickness of *ca.* 11 nm were prepared as follows: PEO- $\text{NH}_2$  (M. W.: 2000) was dissolved in ethanol and the solution was spin-coated on a glass substrate. The films obtained were then heat-treated at 110 °C for 30 min in air to remove residual solvent. The matrix films were set in vacuum evaporator (ULVAC EX-400) and held at 50 °C. High purity metallic iron (99.99 %) was vapor deposited on the molten matrix film from tungsten basket at a pressure of  $<5 \times 10^{-5}$  Torr at a deposition rate of 0.2 nm  $\text{s}^{-1}$  as monitored by a quartz crystal microbalance. The deposition thickness of iron ranged from 100 to 500 nm. The films obtained were then preserved in vacuum chamber for 30 min. Some of the iron deposited matrix films were heat-treated in air to change the particle size.

The size distribution and crystalline structure of the particles were studied by TEM (JEOL JEM-2010) operating at 200 kV. The samples for TEM observations

were prepared by the following procedure; the composites with deposition thickness of iron below 300 nm were dissolved in ethanol and the resultant solutions were dropped onto a copper grid covered by a thin carbon film. In the cases of the composites with deposition thickness of iron above 400 nm, the composites immersed in ethanol were sonicated and immediately mounted onto the copper grid. The content of the resultant particles was determined by TG-DTA, TAS-300 system (Rigaku). The oxidation state of iron in the composites was investigated by XPS with an X-ray photoelectron spectrometer, ESCA 3400 (Shimadzu), using a Mg-K $\alpha$  X-ray source. Crystalline structure of the particles was analyzed by X-ray diffraction measurement (RINT-2100, Rigaku) equipped with thin film attachment. IR spectra were measured using FT-IR (FT/IR 615R, Japan Spectroscopic Co.) in the diffuse reflectance mode to elucidate a structure of PEO-NH<sub>2</sub> in composite. Optical absorption spectra were measured with a UVDEC 660 spectrophotometer (Japan Spectroscopic Co. Ltd.) over the wavelength range 400-800 nm.

### 3. RESULTS AND DISCUSSION

Figure 1 represents TEM images and size distribution of the particles in the composites with 300 nm (a) and 400 nm (b) of the deposited iron thickness. In Fig. 1a, well-dispersed small particles with nearly spherical shape are seen, and their average diameter and standard deviation are *ca.* 1.3 nm and 0.4 nm, respectively. On the other hand, for the composite prepared with 400 nm of the iron deposited thickness (Fig. 1b), the agglomerate of small primary particles with nearly same particle size as those in Fig. 1a is observed. The composite (the thickness of the deposited iron: 300 nm) with well-dispersed particles is soluble in ethanol readily, whereas another one cannot. The content of the resultant particles can be responsible for the difference of their uniform dispersion. The maximum iron oxide content for the dispersed particles (the structure is assumed to Fe<sub>2</sub>O<sub>3</sub> as described later) is *ca.* 10 wt% which is much

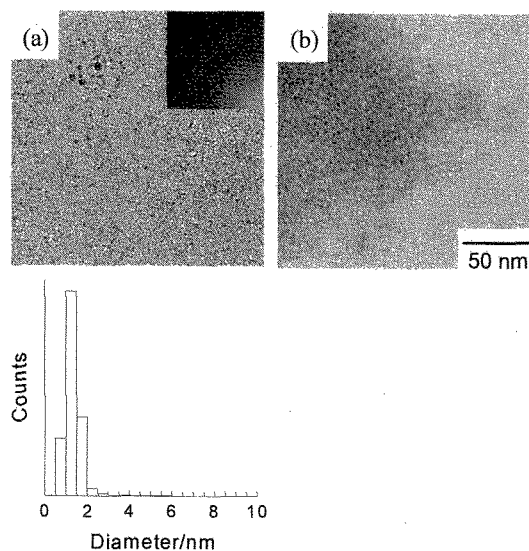


Fig. 1. TEM images and size distribution of the particles obtained by vacuum evaporation of iron onto PEO-NH<sub>2</sub> film. Inset in (a): SAED pattern. The thickness of deposited iron is (a) 300 nm, (b) 400 nm.

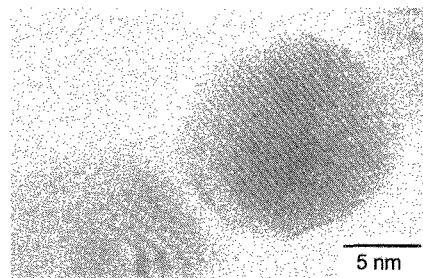


Fig. 2. HRTEM image of  $\alpha$ -Fe<sub>2</sub>O<sub>3</sub> particles obtained by vacuum evaporation of iron onto molten PEO-NH<sub>2</sub> film.

less than that of Cu<sub>2</sub>O system (*ca.* 40 wt%) reported in previous study [17]. This is presumably due to magnetic property of iron.

In the selected area electron diffraction (SAED) pattern, some broad Debye-Scherrer rings were seen (inset in Fig. 1a), indicative of nano-crystalline material. To gain insight into the structure of the particles, HRTEM observation was performed for relatively large particle with *ca.* 8 nm in size. As shown in Fig. 2, the clear lattice fringes can be seen in the HRTEM image, indicating that the particle is single crystal. The *d*-values are accurately measured from the HRTEM image and are consistent with the indices (113) and (024) of corundum  $\alpha$ -Fe<sub>2</sub>O<sub>3</sub> structure. We consider that the oxidation process of the deposited iron is similar with other systems [17, 20]; the initially produced metal iron particles are partially oxidized by the oxygen or water residue in the vacuum chamber and completely oxidized by air when the sample is taken out from the chamber, which is due to the nature of metallic iron to be oxidized easily (because the majority of the particles are less than 8 nm in size). Therefore, the resultant particles may be pure iron oxide.

It is well-known that  $\alpha$ -Fe<sub>2</sub>O<sub>3</sub> is antiferromagnetic but possesses a weak (parasitic) ferromagnetism between Morin temperature and Néel temperature. However, the composite was attracted by hand magnet, despite that the major component is the polymeric matrix (*ca.* 90 wt%), indicative of the existence of ferromagnetic materials ( $\gamma$ -Fe<sub>2</sub>O<sub>3</sub> or Fe<sub>3</sub>O<sub>4</sub>). Fig. 3 shows XPS spectra

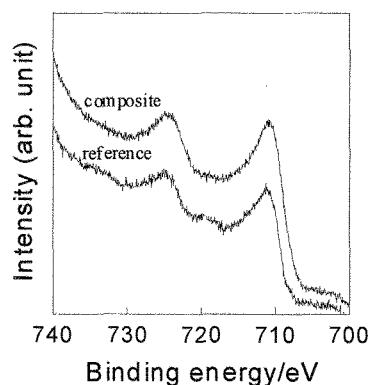


Fig. 3. XP spectra of the Fe 2p core level electrons of the composite and  $\alpha$ -Fe<sub>2</sub>O<sub>3</sub> powder as reference. The composite is prepared by vacuum evaporation of iron onto molten PEO-NH<sub>2</sub> film (the thickness of deposited iron is 300 nm).

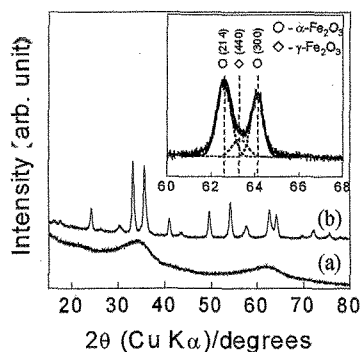


Fig. 4. XRD patterns of the composite as-prepared (a) and heat-treated at 500 °C for 30 min in air (b). (the thickness of deposited iron is 300 nm). Inset figure is a magnified view of the 60-68 degrees region for pattern (b) and decomposition into three components using Gaussian curve fitting program with a non-linear least-square method.

of Fe 2p core-level of the composite (the thickness of the deposited iron: 300 nm) and  $\alpha$ - $\text{Fe}_2\text{O}_3$  powder as a reference. The spectra were corrected using C 1s contamination peak (285.0 eV). The XPS spectrum for the reference showed a main peak at 710.8 eV, which is very similar to the Fe 2p<sub>3/2</sub> level for the  $\text{Fe}^{3+}$  species [21, 22]. The shape of the spectrum and the line positions of the composite coincide with those of reference material. It appears that the surface of nano-sized iron oxide particles is mostly composed of  $\text{Fe}^{3+}$  species. Moreover, iron oxide particles dispersed in the nearly transparent matrix colored to reddish-brown characteristic of nano-sized  $\text{Fe}_2\text{O}_3$  particles [23]. To clarify the existence of  $\gamma$ - $\text{Fe}_2\text{O}_3$ , XRD analysis was performed and the results are shown in Fig. 4. While the as-prepared composite exhibits extensively broad peaks due to very small crystallites (Fig. 4a), Fig. 4b reveals well-characterized sharp peaks for the composite heat-treated at 500 °C, indicating high crystallinity of the sample. Since XRD patterns of  $\gamma$ - $\text{Fe}_2\text{O}_3$  and  $\text{Fe}_3\text{O}_4$  are quite similar, except for the 2 $\theta$  range of 60-68 degrees, the XRD pattern was examined carefully (inset in Fig. 4b). It was confirmed that the structure of iron oxide particles after heat treatment is  $\alpha$ - $\text{Fe}_2\text{O}_3$  and  $\gamma$ - $\text{Fe}_2\text{O}_3$ . Xu et al. reported that heat treatment of nano-sized  $\gamma$ - $\text{Fe}_2\text{O}_3$  particles in air resulted in a transformation to  $\alpha$ - $\text{Fe}_2\text{O}_3$  phase [24], implying that, in the present system, there are large amount of  $\gamma$ - $\text{Fe}_2\text{O}_3$  particles in as-prepared composite.

Metal oxide particles sometimes cause structural

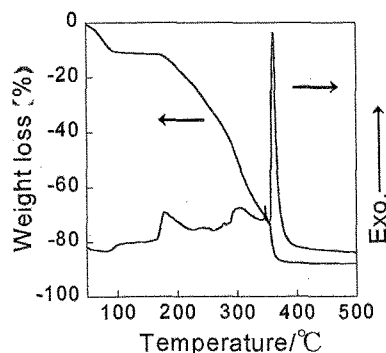


Fig. 5. DTA/TGA curve of the composite. The thickness of deposited iron is 300 nm.

transitions with reducing particle size. Ayyub et al. [25] have reported on the structural transitions of  $\text{Fe}_2\text{O}_3$  particles prepared through chemical route as a function of particle size, in which  $\gamma$ -to- $\alpha$  reconstructive structural transition was confirmed above 30 nm in size, i.e.,  $\gamma$ - $\text{Fe}_2\text{O}_3$  preferentially form for a particle size below 30 nm. They suggested that the size could play the role of a thermodynamic parameter. The critical size for phase transition from  $\alpha$ - $\text{Fe}_2\text{O}_3$  to  $\gamma$ - $\text{Fe}_2\text{O}_3$  is inconsistent with the size of  $\alpha$ - $\text{Fe}_2\text{O}_3$  particle obtained in this study (ca. 8 nm). This may be due to the difference of preparation routes. The majority of as-prepared  $\text{Fe}_2\text{O}_3$  particles may consist of  $\gamma$ -phase because not only the mean diameter (1.3 nm) is much less than 8 nm but also the size distribution is fairly narrow. This consideration is supported from the phenomena that composite is attracted by hand magnet. It is concluded that  $\alpha$ - and  $\gamma$ - $\text{Fe}_2\text{O}_3$  particles coexist in the composite (presumably main component of as-prepared particles is  $\gamma$ - $\text{Fe}_2\text{O}_3$ ).

The present preparation technique is very simple process and the composite obtained is easy to handle as a solid with a wax-like texture at room temperature. In addition, the composite is readily soluble in useful solvents such as water and ethanol for industry applications. The composite and its solution are very stable at room temperature with no indicative of aggregation or coalescence for nano-sized  $\text{Fe}_2\text{O}_3$  particles over several weeks. Consequently, we believe that the particles can be utilized for a starting material in a variety of applications.

Physical and chemical properties of nano-sized particles are often influenced by their particle size and hence the size control is objective of intense research. To determine heat treatment temperature to induce particle growth, thermal stability of the composite was studied by TG-DTA analysis. Typical TG-DTA curve of the composite (thickness of deposited iron: 300 nm) is depicted in Fig. 5. It showed a rapid drop in weight at near room temperature accompanied by broad endothermic band, followed by a gradual monotonic decrease in weight at higher temperature with some exothermic bands. Other composites with different content of iron oxide also exhibited same tendency. The structure of PEO-NH<sub>2</sub> in the composite after heat treatment was characterized by FT-IR study (not shown) so that no structural change was confirmed by heat treatment below 130 °C, indicating that the weight loss below 130 °C is due to vaporization of water included in the composite. Therefore, we performed heat treatment below 130 °C in order to vary  $\text{Fe}_2\text{O}_3$  particle size.

Figure 6 represents TEM images and size distribution of  $\text{Fe}_2\text{O}_3$  particles heat-treated at 110 °C (a) and 130 °C (b) for 24 h. When the composite was heat-treated at 110 °C, well-dispersed particles with relatively narrow size distribution were observed and the average diameter increases from 1.34 nm to 3.51 nm. At 130 °C, further particle growth proceeded as shown in Fig. 6b (the particle diameter cannot be estimated correctly, since the particles considerably aggregate). However, the corresponding SAED pattern (inset in Fig. 6b) mostly remains unchanged, as compared to that of as-prepared one (see Fig. 1a). This means that the relatively large particles are composed of primary  $\text{Fe}_2\text{O}_3$  nanoparticles seen in Fig. 1a. Figure 7 shows optical absorption spectra for these composites dissolved in ethanol. It is important to note that the as-prepared

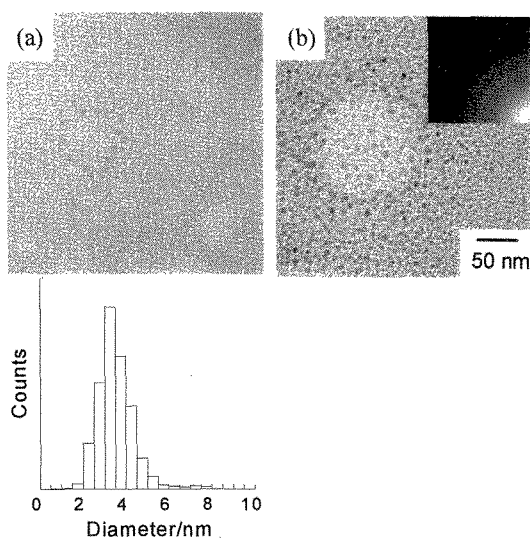


Fig. 6. TEM images and size distribution of  $\text{Fe}_2\text{O}_3$  particles dispersed in PEO-NH<sub>2</sub> after heat treatment at 110 °C (a) and 130 °C (b) for 24 h. Inset in (b): SAED pattern. The thickness of deposited iron is 300 nm.

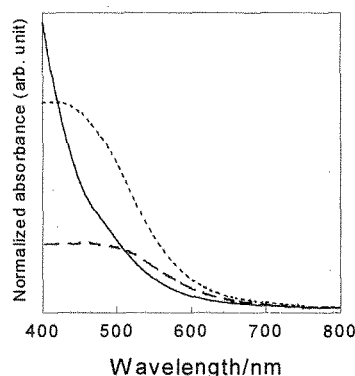


Fig. 7. Optical absorption spectra of  $\text{Fe}_2\text{O}_3$  particles dispersed in PEO-NH<sub>2</sub> after heat treatment. The thickness of deposited iron is 300 nm.

Heat treatment condition: (—) non, (---) 110, (- · -) 130 °C

$\text{Fe}_2\text{O}_3$  particles absorb little in the visible spectral region, presumably due to their nanometer size [26]. The absorption edge of  $\text{Fe}_2\text{O}_3$  particles shifts to longer wavelength with increasing particle size. This demonstrates that the optical property of  $\text{Fe}_2\text{O}_3$  particles can be controlled by varying the heat treatment temperature.

#### 4. CONCLUSION

By using a vacuum evaporation technique, nano-sized  $\text{Fe}_2\text{O}_3$  particles with relatively narrow distribution have been prepared successfully. The particles uniformly dispersed in PEO-NH<sub>2</sub> film with no evidence for significant aggregation up to 10 wt% of  $\text{Fe}_2\text{O}_3$  content. From HRTEM observation, XPS and XRD measurements, it was elucidated that the composites contain the mixture of pure  $\alpha$ - and  $\gamma$ - $\text{Fe}_2\text{O}_3$ . The composites were very stable and dissolved in water and ethanol with no evidence for aggregation. The particle

diameter is controllable with varying heat treatment temperature, which is due to aggregation of primary  $\text{Fe}_2\text{O}_3$  particles. It induces to the continuous shift of an absorption edge of  $\text{Fe}_2\text{O}_3$  particles in optical spectrum toward longer wavelength. We believe that the present composites and its solution enable us to use for a variety of applications, e.g., catalysis, magnetic storage media, ferrofluid, and optical device.

#### REFERENCES

- [1] G. A. Ozin, *Science*, **271**, 920-922 (1996).
- [2] J. H. Flender, *Chem. Rev.*, **87**, 877-899 (1987).
- [3] A. Henglein, *Chem. Rev.*, **89**, 1861-1873 (1989).
- [4] V. L. Colvin, M. C. Schlamp, A. P. Alivisatos, *Nature*, **370**, 354-357 (1994).
- [5] G. Schmid, *Chem. Rev.*, **92**, 1709-1727 (1992).
- [6] B. C. Gates, *Chem. Rev.*, **95**, 511-522 (1995).
- [7] A. F. Lee, C. J. Baddeley, C. Hardacre, R. M. Lambert, G. Schmid, H. West, *J. Phys. Chem.*, **99**, 6096-6102 (1995).
- [8] Y. S. Kang, S. Risbud, J. F. Rabolt, P. Stroeve, *Chem. Mater.*, **8**, 2209-2211 (1996).
- [9] T. Prozorov, A. Gedanken, *Adv. Mater.*, **10**, 532-535 (1998).
- [10] B. A. Tang, Y. Geng, J. W. Y. Lam, B. Li, X. J. X. Wang, F. Wang, A. B. Pakhomov, X. X. Zhang, *Chem. Mater.*, **11**, 1581-1589 (1999).
- [11] K. V. P. M. Shafi, A. Ulman, X. Yan, N-L. Yang, C. Estournès, H. White, M. Rafailovich, *Langmuir*, **17**, 5093-5097 (2001).
- [12] P. D. A. Basumallick, *Appl. Surf. Sci.*, **182**, 398-402 (2001).
- [13] J. H. Jean, T. A. Ring, *Langmuir*, **2**, 251-255 (1986).
- [14] N. Mounien, M. P. Pileni, *Chem. Mater.*, **8**, 1128-1134 (1996).
- [15] S. Grimm, M. Schultz, S. Barth, R. Müller, *J. Mater. Sci.*, **32**, 1083-1092 (1997).
- [16] S. Deki, K. Sayo, A. Yamada, K. Akamatsu, S. Hayashi, *J. Colloid Interface Sci.*, **214**, 123-125 (1999).
- [17] H. Yanagimoto, K. Akamatsu, K. Gotoh, S. Deki, *J. Mater. Chem.*, **11**, 2387-2389 (2001).
- [18] R. M. Cornell and U. Schwertmann, "The Iron Oxides" VCH Verlagsgesellschaft mbH, Weinheim, Germany (1996).
- [19] F. A. Cotton and G. Wilkinson, "Advanced Inorganic Chemistry — A Comprehensive Text" Interscience, 4th ed., New York (1962) p. 752.
- [20] T. Masui, K. Machida, T. Sakata, H. Mori, G. Adachi, *J. Alloys&Compd.*, **256**, 97-101 (1997).
- [21] N. S. McIntyre, D. G. Zetaruk, *Anal. Chem.*, **49**, 1521-1529 (1977).
- [22] C. Palacio, A. Arranz, *J. Phys. Chem. B*, **105**, 10805-10811 (2001).
- [23] Y. S. Kang, S. Risbud, J. F. Rabolt, P. Stroeve, *Chem. Mater.*, **8**, 2209-2211 (1996).
- [24] X. N. Xu, Y. Wolfus, A. Shaulov, Y. Yeshurun, *J. Appl. Phys.*, **91**, 4611-4616 (2002).
- [25] P. Ayyub, M. S. Multani, M. Barma, V. R. Palkar, R. Vijayaraghavan, *J. Phys. C*, **21**, 2229-2245 (1988).
- [26] R. F. Ziolo, E. P. Emmanuel, B. A. Weinstein, M. P. O'Horo, B. N. Ganguly, V. Mehrotra, M. W. Russell, D. R. Huffman, *Science*, **257**, 219-223 (1992).

(Received December 20, 2002; Accepted March 1, 2003)